

Trigger characteristics of torrential flows from high to low alpine regions in Austria

Prenner, D.; Hrachowitz, M.; Kaitna, R.

DOI

[10.1016/j.scitotenv.2018.12.206](https://doi.org/10.1016/j.scitotenv.2018.12.206)

Publication date

2019

Document Version

Final published version

Published in

Science of the Total Environment

Citation (APA)

Prenner, D., Hrachowitz, M., & Kaitna, R. (2019). Trigger characteristics of torrential flows from high to low alpine regions in Austria. *Science of the Total Environment*, 658, 958-972.
<https://doi.org/10.1016/j.scitotenv.2018.12.206>

Important note

To cite this publication, please use the final published version (if applicable).
Please check the document version above.

Copyright

Other than for strictly personal use, it is not permitted to download, forward or distribute the text or part of it, without the consent of the author(s) and/or copyright holder(s), unless the work is under an open content license such as Creative Commons.

Takedown policy

Please contact us and provide details if you believe this document breaches copyrights.
We will remove access to the work immediately and investigate your claim.

Green Open Access added to TU Delft Institutional Repository

'You share, we take care!' - Taverne project

<https://www.openaccess.nl/en/you-share-we-take-care>

Otherwise as indicated in the copyright section: the publisher is the copyright holder of this work and the author uses the Dutch legislation to make this work public.



Trigger characteristics of torrential flows from high to low alpine regions in Austria

D. Prenner^{a,*}, M. Hrachowitz^b, R. Kaitna^a

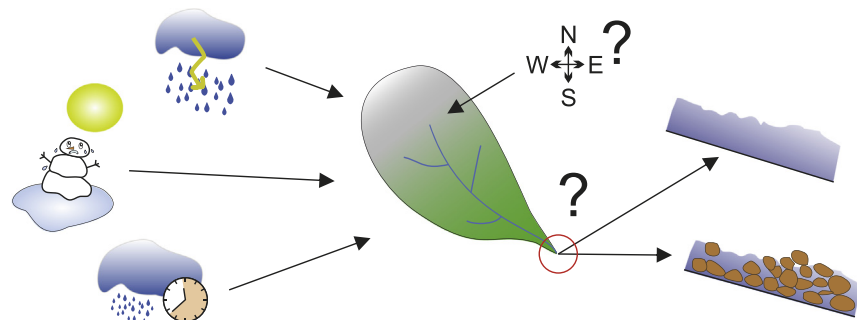
^a Institute of Mountain Risk Engineering, University of Natural Resources and Life Sciences, Vienna, Austria

^b Water Resources Section, Faculty of Civil Engineering and Geosciences, Delft University of Technology, the Netherlands

HIGHLIGHTS

- We identify hydro-meteorological trigger conditions for torrential flows
- Triggering precipitation varies with trigger type and type of flow
- Regional wetness states are significantly different for each trigger
- Watershed relief and orientation play a role for specific trigger types

GRAPHICAL ABSTRACT



ARTICLE INFO

Article history:

Received 24 September 2018

Received in revised form 29 November 2018

Accepted 13 December 2018

Available online 15 December 2018

Editor: Ralf Ludwig

Keywords:

Debris flows

Fluvial flows

Trigger

Hydrology

Geomorphology

ABSTRACT

Torrential processes like fluvial flows (flash floods with or without intensive sediment transport) and debris flows can represent a threat to people and infrastructure in alpine domains. Up to now the hydro-meteorological trigger conditions and their connection with geomorphic watershed characteristics that favor the initiation of either process are largely unknown. Based on modeled wetness states we determined the trigger types (long-lasting rainfall (LLR), short-duration storm (SDS) and intense snow melt (SM)) of 360 observed debris flow and fluvial flood events in six climatically and geomorphologically contrasting watersheds in Austria. Results show that the watershed wetness states play very distinct roles for triggering torrential events across the study regions. Hydro-meteorological variables have little power to explain the occurrence of fluvial flows and debris flows in these regions. Nevertheless, trigger type separation highlighted some geomorphic influences. For example, intense SM triggered more events in sub-watersheds (torrential watersheds in the study region) that are characterized by significantly higher Melton ruggedness numbers than LLR does. In addition, the data show that events triggered by LLRs occur in sub-watersheds of similar exposures (aspects) other than SDS. The results suggest that the consideration of different trigger types provides valuable information for engineering risk assessment.

© 2018 Elsevier B.V. All rights reserved.

1. Introduction

Extreme water input from rainfall or intense snow melt into head-water mountain watersheds frequently induces geomorphological responses in torrential channels that can range from (flash) floods, bed load transport to debris flows (Merz and Blöschl, 2003; Borga et al.,

* Corresponding author.

E-mail address: david.prenner@boku.ac.at (D. Prenner).

2014). In the long run, these torrential processes contribute to landscape evolution (Stock and Dietrich, 2003), but also can represent a threat to human lives, settlements, and infrastructure immediately at their occurrence (Ballesteros Cánovas et al., 2016; Fuchs et al., 2017). An important task for natural hazard management is to identify watersheds prone to torrential activity as well as which type of process is expected to occur for a certain watershed under varying hydro-meteorological conditions in order to provide a high level of protection for endangered communities.

Studies of the alluvial fan of torrential watersheds turned out to be valuable for alpine hazard assessment as it enables a delineation of flow process. Initially, Melton (1957) found a connection between the fan slope of a torrential watershed and the relief of the watershed what is expressed by Melton Ruggedness Number that is a function of the watersheds elevation range and its area. Later, Jackson et al. (1987) successfully applied the Melton Ruggedness Number to distinguish between debris flow fans and fluvial fans in the Canadian Rockies since the fan of debris flow active watersheds emerged to be significantly steeper than of one with fluvial dominating processes. Heiser et al. (2015) used the Melton Ruggedness Number to separate between floods, bed load transport, and debris flows as a dominant torrential process. However, Scheidl and Rickenmann (2009) report of watersheds where different geomorphological movements occur even during the same rainstorm event, which indicates that relief is not sufficient to predict the dominant torrential process type.

Another commonly used watershed attribute for landslide susceptibility assessments (of which debris flows are part of according to the definition of Hungr et al., 2014), is slope aspect (Capitani et al., 2013), although there is an ongoing discussion about its significance. While Galli et al. (2008) and Yalcin et al. (2011) found that the use of aspect improves landslide susceptibility mapping, other studies come to an opposite conclusion and report no significant influence of aspect onto results (Luzi and Pergalani, 1999; Ayalew et al., 2004). Atkinson and Massari (1998) differentiate between dormant and active landslides and report that aspect has explanatory power only for dormant slopes. According to the authors, recently active landslides in their study regions were “generally shallow surface features”, which occur distributed over all aspects. Capitani et al. (2013) concluded that the unclear role of aspect emerges from an occasionally occurring correlation of aspect with other, unconsidered variables (e.g. geological fault zone) that would explain the susceptibility for landslide better.

Besides morphological evidence, less is known about the impact of different meteorological conditions (trigger types) for the generation of a geomorphological response in the channel. On the regional scale, empirical thresholds of rainfall characteristics (mostly intensity-duration thresholds) have been derived for predicting at which level of water input a watershed response causes the formation of debris flows or bed load transport (e.g. Guzzetti et al., 2008; Berti et al., 2012; Badoux et al., 2012). These meteorological thresholds show considerable regional differences and uncertainties. Therefore different studies tried to capture the effect of the hydrological history of a watershed on the channel runoff (e.g. Merz and Blöschl, 2003; Borga et al., 2014) and debris flow initiation (e.g. Glade et al., 2000; Borga et al., 2014; Bogaard and Greco, 2016). Mostbauer et al. (2018) found a varying influence of different sources of water (precipitation, soil moisture, snow melt) at debris flow initiation by analyzing hydro-meteorological variables gained from a hydrological model. In a following work, Prenner et al. (2018) analyzed multiple hydro-meteorological watershed variables and found that distinct watershed states exist when debris flows occur. These distinct watershed states reflect the existence of different meteorological trigger types, which were classified as long-lasting rainfall events (LLR), short-duration storms (SDS) and events associated with snow melt (SM).

On the hillslope-channel scale, several studies address the development of a geomorphic response in small mountain basins due to rainfall input (e.g. Johnson and Sitar, 1990; Marchi et al., 2002). Recently, Kean

et al. (2013) and McGuire et al. (2017) presented a hydro-geomorphic model to describe the runoff formation and sediment dynamics in recently burned watersheds. Doing this, the authors conclude that debris flow surges origin from periodic deposition and release of sediment in the channel rather than from channel bank failure or continuous erosion of grains from the bed. Gregoretti and Fontana (2008) reconstructed channel runoffs at debris flow occurrence from precipitation gauges, to study their initiation mechanism due to channel bed erosion.

In this work, we are interested in the regional variation of hydro-meteorological triggering conditions (LLR, SDS, SM) for debris flows and fluvial flows (floods that may include intensive bed-load transport) and characteristics of the sub-watersheds (as we refer to the torrential watersheds of the study region) in which trigger types initiate flows. For determination of the trigger conditions, we apply the methodology presented in Prenner et al. (2018) for debris flows that bases on the analysis of multiple hydro-meteorological variables (precipitation, evapotranspiration, soil moisture, snow melt rate, etc.) derived from a hydrological model. For this study we hydrologically modeled six contrasting regions in the Austrian Alps on a daily basis starting around 1950 and connect it to documented debris flow and fluvial flow events in sub-watersheds. We hypothesize that (1) hydro-meteorological trigger conditions generally differ for debris flows and fluvial flow processes, (2) trigger conditions vary between different regions in the Austrian Alps, and (3) trigger conditions vary with geomorphic basin characteristics (aspect and relief) within the same region.

2. Study regions

We chose contrasting study regions in the Austrian Alps (Fig. 1). From west to east the regions are the Montafon (west), Pitztal (west), Defereggental (south) Gailtal (south), Paltental (east) and Feistritzal (east). The regions differ according to their dominant climatic influences (oceanic-west, Mediterranean-south, and continental-east), topography as well as data availability and a number of observed torrential flow events. The western and southern watersheds (Fig. 1A–D) are of alpine (2100–2700 m) to subalpine character (1400–2100 m) with some glacial influence (except the Gailtal, Fig. 1D), whereas the eastern regions are situated in the montane zone (800–1400 m) and below according to the classification for the central alps after Ellenberg et al., 2010. Metamorphic rocks dominate the geology in the most regions (above 80%); only the Paltental (60% of meta-sedimentary rocks) and the Gailtal (13% sedimentary, 17% meta-sedimentary) are more complex.

According to the Hydrological Atlas of Austria (Nachtnebel, 2003), the comparatively wettest watershed is the Montafon region with a mean annual precipitation of 1548 mm. In contrast, the Feistritzal is the driest with 910 mm/year. Runoff coefficients decrease from the west towards the eastern regions: the Montafon, Pitztal, Defereggental have the highest runoff coefficients 0.78–0.79, followed by Gailtal (0.67) and Paltental (0.63) and the most eastern, the Feistritzal (0.38). This may be partly explained by the higher fraction of forest and grassland in the eastern regions, which increases the water retention capacities of the watersheds. On the contrary, sparsely vegetated/bare rock domains are dominating much of the western watersheds Montafon, Pitztal, and Defereggental.

The region with the highest number of days with documented torrential events is the Montafon with 57 days, followed by the Paltental (29), Gailtal (23), Defereggental (22), and the Pitztal and Feistritzal with 14 event days each. In the two most western regions, Montafon and Pitztal, the number of debris flow event days exceed the number of fluvial flow event days. This is reverse to the four other study regions, where more fluvial flow than debris flow event days were registered. In all regions, we find sub-watersheds which experienced both, debris flows and fluvial flows. A detailed summary of the characteristics and event history of the study region are given in Table 1.

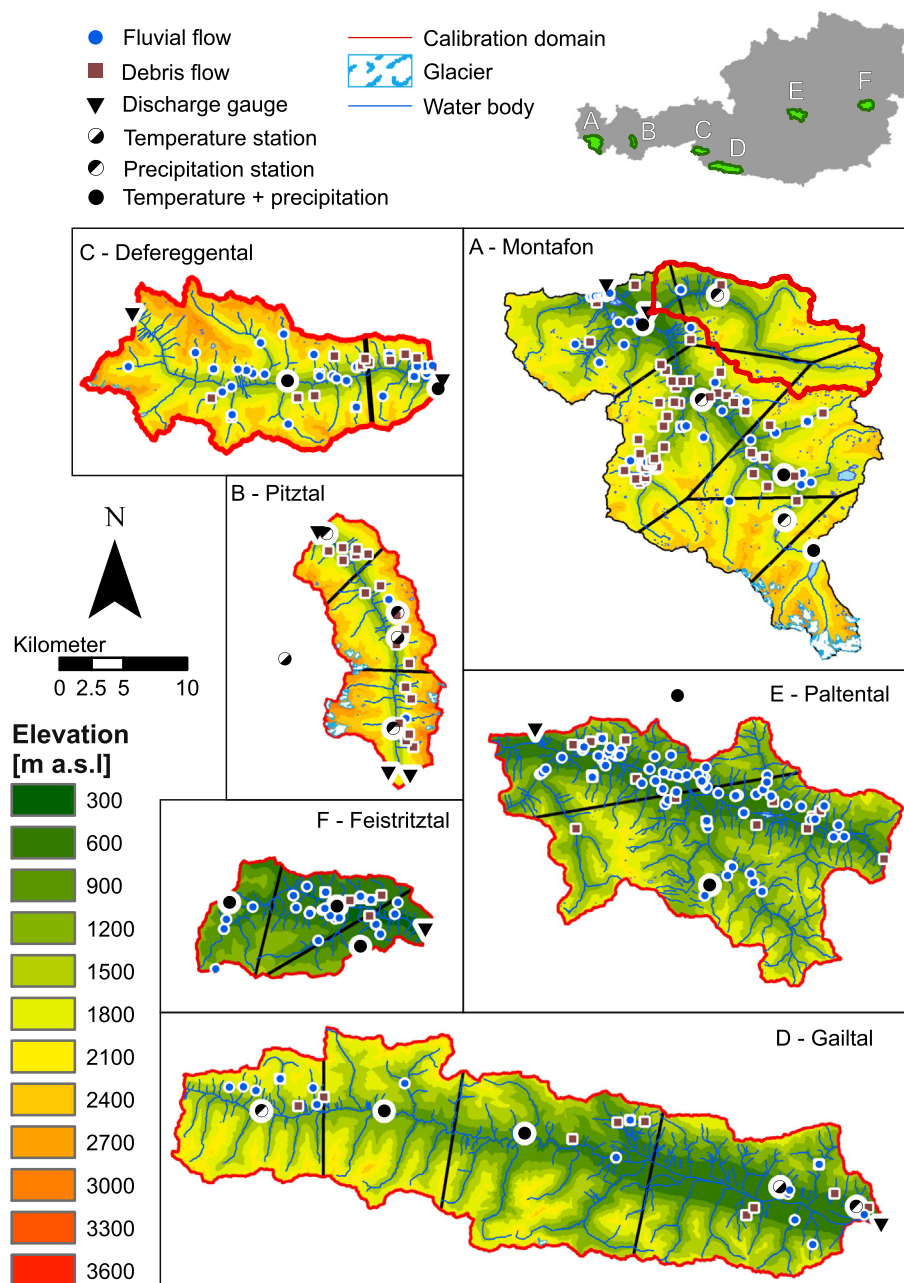


Fig. 1. Overview of the six study regions Montafon (A), Pitztal (B), Defereggental (C), Gailtal (D), Paltental (E) and the Feistritzal (F) (from west to east), the location of documented torrential events (debris flows or fluvial flows), precipitation, temperature and runoff measurement stations, glaciers, water bodies and elevation distribution. Precipitation zones (based on a Thiessen polygon decomposition using the locations of available rain gauges) are marked with black-colored edges.

3. Methods

3.1. Available data

The hydrological model runs of the six study regions are based on daily station data of precipitation, temperature (minimum, maximum, mean) and runoff, which are operated by the Austrian Central Institute for Meteorology and Geodynamics (ZAMG), Hydrographic Service Austria (HD) and its provincial subdivisions, hydropower plant companies Illwerke AG and Tiwag AG (see Fig. 1). HD operated stations provide temperature recordings at 7 am, 2 pm and 9 pm, from which we derived daily mean temperature using the Kaemtz-method in Dall'Amico and Hornsteiner (2006). Daily precipitation sums were calculated at 7 am each day. Runoff data was available at 15 min timesteps and transferred into daily sums according to the reference time for

summation of the precipitation data from 7 am to 7 am. Further input data for the hydrological model was the CORINE Land Cover dataset from 1990, a 10×10 m digital elevation model (vogis.cnv.at), a 10×10 m height-above-nearest drainage map (HAND) (Rennó et al., 2008) and a glacier distribution map (Patzelt, 2015).

For each study region past torrential flow events in the sub-watersheds were available from a database assembled by Hübl et al. (2008a, 2008b, 2008c, 2010) from different historical sources. The authors differentiated between four flow process types based on described morphologic evidence and eyewitness reports. Hardly any measurements of flow characteristics or composition are available. A rough indication of the volumetric sediment concentration c_s can be found in the Austrian Standards International (2009). Floods and fluvial sediment transport commonly show c_s values up to 0.2 while debris flows usually are expected to have a c_s value > 0.4 . The category debris flood with 0.2

Table 1

Characteristics of the six study regions.

Sources: ¹Nachtnebel (2003), ²Mader et al. (1996).

	Montafon	Pitztal	Defereggental	Gailtal	Paltental	Feistritzal
Area [km ²]	510	133	222	586	368	115
Available rain gauges [#]	6	3	2	4	2	3
Mean area per rain gauge [km ²]	85.0	44.3	111.0	146.5	184.0	38.3
Yearly mean precipitation ¹ [mm/yr]	1548	1151	1300	1410	1337	910
Yearly mean runoff coefficient ¹ [–]	0.79	0.78	0.79	0.67	0.63	0.38
River regime ²	Nivo-glacial (nival at Litzbach)	Nivo glacial	Nival	Autumn-nival	Moderate nival	Nivo-pluvial
Elevation range (mean elevation)	631–3312 (1877)	1093–3527 (2238)	1095–3398 (2171)	596–2780 (1477)	634–2446 (1316)	451–1593 (918)
[m a.s.l.]						
Fraction sedimentary rocks [%]	6	0	0	0	13	20
Fraction metamorphic rocks [%]	90	100	83	37	70	80
Fraction meta-sedimentary rocks [%]	4	0	1	60	17	0
Fraction volcanic rocks [%]	0	0	16	3	1	0
Fraction bare rock/sparsely vegetated (glacier share) [%]	31 (2)	51 (3)	39 (0.2)	7 (0)	2 (0)	0 (0)
Fraction grassland [%]	39	26	30	33	48	24
Fraction forest [%]	26	22	28	57	46	71
Fraction riparian zone [%]	4	1	3	3	4	5
Model period	1953–2013	1967–2013	1945–2016	1950–2013	1961–2013	1957–2013
Calibration period	1976–2011	1986–2010	1982–1986	1976–2005	1976–1999	1995–2011
Validation period	2012–2013	2011–2012	1987	2006–2007	2000–2001	2012–2013
Total event days	57	14	22	23	29	14
Fluvial flow event days [#]	22	3	15	18	22	12
Debris flow event days [#]	43	13	10	10	12	3

$< c_s < 0.4$ represents a transition process between fluvial flows and debris flows. Since the number of events documented as debris floods is low and to allow for a better separation, we excluded debris floods from our analysis. Another uncertainty arises from the definition of fluvial flows. Historically these flood events were documented only because of the damage caused by water runoff or sediment deposition outside of the channel. Smaller floods that did not overtop the channel banks were not documented. Due to the lack of data in such small basin, there is no information about the magnitude or return period.

For all sub-watersheds that experienced a documented flow event, mean aspect and Melton Ruggedness Number (elevation difference of the watershed divided by square root of the watershed area) were computed from the DEM.

3.2. Hydrological model

A hydrological model was set up and run for each study region to obtain estimates of system state and flux variables such as soil moisture, snow melt, evapotranspiration or runoff besides the meteorological quantities of precipitation and temperature necessary for event trigger identification as well as analysis about the temporal development of watershed state before events. Therefore we use a semi-distributed, conceptual rainfall-runoff model, which was introduced in (Prenner et al., 2018). Since multiple rain gauges were available for every region, a Thiessen-Polygon decomposition (separation of representative areas for different rain gauges, see Thiessen, 1911) of the study regions were used to delineate the areal influence of each station (in the following referred to as precipitation zones). In case when temperature was not measured at the rain gauge locations, we use the closest temperature station available to compensate the missing data. Depending on the available data, the model periods range from 1953 to 2013 for the Montafon region, 1967–2013 for the Pitztal, 1945–2016 for the Defereggental, 1950–2013 for the Gailtal, 1961–2013 for the Paltental and 1957–2013 for the Feistritzal (Table 1).

The heterogeneous hydrological response from different land-use and topographic characteristics was considered by creating four hydrological response units (HRU) of bare rock/sparsely vegetated areas, forest, grassland and riparian zones (e.g. Gao et al., 2014). While the first three HRUs represent steeper, hillslope domains, the riparian zone accounts for hydrologically quick responding zones close to surface waters, which we determined by a HAND value of smaller than 3 m (cf.

Gharari et al., 2011). The elevation range of each HRU was discretized into bands of 100 m to account for altitude dependent quantities like precipitation and temperature (by using altitude depended correction factors) and thereof related evapotranspiration, melt and glacier dynamics (Sevruk, 1997; Rolland, 2003). The presence of glaciers in bare rock domains is modeled as an unlimited water supply for their share they hold in an elevation zone (e.g. Gao et al., 2017). Each HRU in each precipitation zone is represented by an individual set of reservoirs for snow, glacier (active only bare rock/sparsely vegetated domain), interception, soil and fast responding surface and sub-surface. Differently, the groundwater dynamics are modeled with a single reservoir for all HRUs of a precipitation zone (Euser et al., 2015).

All computed quantities from HRUs and elevation bands are transformed by arially weighting to the precipitation zone scale, which equals the highest resolution of available precipitation information and is therefore our working scale for the hydro-meteorological analysis. However, the modeled runoff is further upscaled from the precipitation zone scale to the watershed scale (also by area-weight) and represents the total runoff for model calibration.

For model calibration, we applied the likelihood-based differential evolution adaptive metropolis sampler (DREAM) to obtain the posterior distributions of the 43 calibration parameters (Vrugt et al., 2008; Vrugt, 2016). Uncertainties from the hydrological modeling were considered by simulating each region with 100 different model parameter sets, randomly sampled from the parameters posterior distributions. Model performance was, post-calibration, evaluated by performance metrics Nash-Sutcliffe Efficiency of flow (NSE; Nash and Sutcliffe, 1970), NSE of the logarithm of flow (logNSE), the Volumetric Efficiency of flow (VE; Criss and Winston, 2008) as well as the NSE for the flow duration curve (FDNSE). All these measures were combined in the Euclidean distance D_e (Eq. 1), which states the overall model performance as degree of deviation from the optimal value of zero (e.g. Hrachowitz et al., 2014).

$$D_e = \sqrt{(1 - \text{NSE})^2 + (1 - \log\text{NSE})^2 + (1 - \text{VE})^2 + (1 - \text{FDNSE})^2} \quad (1)$$

The calibration and independent validation periods for each region are given in Table 1. For model warm-up we use the two years which precede the calibration period. Model structure including fluxes and

reservoirs and the model water balance equations are provided in the supplementary material A.

3.3. Trigger identification

The identification of the trigger of the historical debris flow and fluvial flow events is based on a holistic analysis of the temporal development of watershed state before event occurrence following the approach from an exploratory study presented in Prenner et al., 2018. By this method, we use multiple quantitative criteria to capture characteristic hydro-meteorological signals for the different trigger types long-lasting rainfall LLR, short-duration storms SDS and intense snow melt SM. In Fig. 2 we present a decision tree according to which watershed states were linked to a certain trigger. Note that avoiding, to some degree, the epistemic uncertainties from point precipitation measurements and exploiting the low-pass filter properties of watersheds (e.g. Euser et al., 2015), precipitation is here not directly used as a criterion. Instead, as demonstrated by Prenner et al. (2018), we assume that the combination of increasing soil moisture and decreasing potential evapotranspiration prior to an event-day, together with a narrow temperature span at the event day, is an indication that a LLR triggered an event. On the contrary, a decrease of soil moisture, increase of potential evapotranspiration and a large temperature span are observations typical for SDS. Finally, we interpret an intense modeled snow melt as a SM trigger. To avoid an a priori definition of so called “hard” thresholds for each criterion, threshold values were sampled a 1000 times from a uniform distribution, bounded by two plausible, representative percentiles of the value range of a hydro-meteorological variable. The trigger mechanism assigned for each torrential event was then the most frequent mechanism identified. Hydrological uncertainties are considered by alternately sampling from one of the 100 simulation runs. For trigger determination, all precipitation zones of a study region were analyzed and not just that zone where the torrential event occurred as it was done in Prenner et al. (2018). Like that we prevent the (probably theoretically) case that for events at the same day but in different precipitation zones, diverging trigger types are obtained. The determined trigger types are further cross-checked for plausibility with weather reports from the Austrian Central Institute for Meteorology and Geodynamics (ZAMG) available since 1999. Since reports do not clearly state the type of trigger

condition (LLR, SDS or SM), we linked reported low-pressure systems to LLR and high-pressure systems and convective rainfall events to SDS.

3.4. Statistical testing

For testing statistical significance that events grouped by their trigger type (LLR, SDS or SM) or between event types (fluvial flows or debris flows) emerge from different populations, we use the Wilcoxon rank sum test (Wilcoxon, 1945).

3.5. Watershed aspect trigger probabilities

The Bayesian theorem (Bayes and Price, 1763) in Eq. (2) is applied for analyzing the relationship between trigger type T (LLR; SDS, SM) and the mean aspect A (north azimuth: 315° – 45° , east: 45° – 135° , south: 135° – 225° , west: 225° – 315°) of the sub-watersheds where events were observed.

$$P(A|T) = \frac{P(A) * P(T|A)}{P(T)} \quad (2)$$

The term $P(A|T)$ reflects the posterior probability that an event is triggered in a watershed of aspect A by the trigger T . Probability $P(A)$ designates the prior knowledge that a certain aspect is affected by a torrential event, independent of the responsible trigger. $P(T|A)$ expresses the likelihood that a certain trigger T already occurred at a sub-watershed of mean aspect A . The denominator term represents the marginal probability $P(T)$, which acts as a scaling variable so that the posterior probability $P(A|T)$ for all four aspects integrate to unity. A strong deviation of the posterior probability $P(A|T)$ from the prior probability $P(A)$ suggests, that the information about trigger type T adds significant new knowledge.

4. Results

4.1. Hydrological model

Results suggest that the hydrological system dynamics of all six study regions were reproduced satisfactorily for the calibration period as well as for the subsequently starting independent validation period

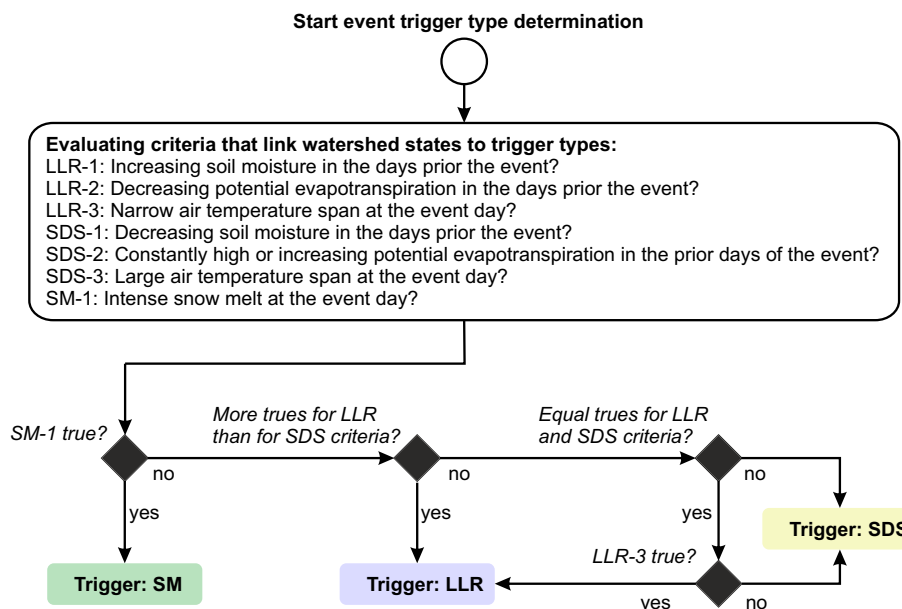


Fig. 2. Decision tree according to which a watershed state at and prior the event day was linked to a certain trigger LLR, SDS or SM. For details about the methodology, the deviation of the criteria and corresponding thresholds please see Prenner et al. (2018).

by the model (see Table 2). While best performances were achieved in the regions Pitztal (D_E , calibration = 0.23, D_E , validation = 0.24) and Defereggental (D_E , calibration = 0.24, D_E , validation = 0.26), the regions Paltental (D_E , calibration = 0.50, D_E , validation = 0.27) and Montafon (D_E , calibration = 0.43, D_E , validation = 0.41) achieved weaker performances. A manual inspection of the simulation results manifests some weaknesses in modeling snow melt dynamics, which could be explained by the implementation of a simplified degree-day model (Hock, 2003) as well as the underestimation of precipitation when it occurs as snow fall (Parajka et al., 2005). Nevertheless, the models were almost completely able to reproduce the river regimes of the study watersheds as they were characterized by (Mader et al., 1996). Only one minor deviation was observed for the Pitztal, where the month of modeled peak flow is in June rather than as observed July. We explain this effect with deficits of modeling glacial zones upstream of the simulation domain, which would provide the water input for July due to the melting of ice (see Fig. 1).

In Fig. 3a, we exemplarily show measured and modeled hydrological variables of the Pitztal region for the event year 2010 to get an overview about the hydrological system. In Fig. 3b–d, we provide a detailed view on the watershed state around the occurrence of three selected torrential events in the same region. For the event on 6th August 1985 (Fig. 3b) a high precipitation intensity (above 50 mm d^{-1}) was recorded on the event day in connection with a low temperature span. Since soil moisture increased due to ongoing rainfall and air temperature falls over the prior days we interpret this event being triggered because of LLR. An example for a SDS trigger is the event on the 11th July 2010 (Fig. 3c). Here precipitation intensity on the event day was in the medium range (about 30 mm d^{-1}) and soil becomes drier due to evapotranspiration facilitated by high temperatures in the days before. Almost no rainfall was observed with the event on the 20th May 1979 but rather a high snow melt above 20 mm d^{-1} pointing to a trigger of SM (Fig. 3d). Overviews about the hydrological system at torrential event occurrence of the remaining study regions can be found in the supplementary material B.

4.2. Identification of triggers and their temporal and regional occurrence characteristics

We find that over all regions debris flow and fluvial flow events were triggered mostly by SDS (87 event days), followed by LLR (60 event days) and SM (12 event days SM). There is a varying dominance of trigger types across the regions as displayed in Fig. 4. While in the Montafon torrential events were triggered preferentially by SDS (34 SDS to 18 LLR event days), it is reverse in the Gailtal, where LLR is slightly in the dominant trigger (10 SDS to 11 LLR event days). Events triggered by SM appeared in every region except the low-altitude region

Feistritzal. In most regions, debris flows tend to be triggered preferentially by SDS rather than LLR. Fluvial flows are a more equally distributed between trigger types SDS and LLR. The detailed classification results including the trigger-type probabilities for the six study regions are shown in supplementary material C.

Besides spatial differences, there is also a seasonal pattern for the occurrence of specific trigger types (Fig. 5). Event days on which at least one torrential flow was observed occurred in 10 out of 12 months (except January, February) across all regions. Reflecting results of Mostbauer et al. (2018), intense SM trigger appeared comparatively clustered in May (54% of all SM event days), followed by June (23%) and April (15%). A similar cluster is visible for SDS trigger, which favorably occur in July, representing 48% of all event days of this trigger type. Interestingly, the preference for SDS to occur in the rainiest month July (except the Feistritzal) decreases from the western to eastern regions—56% and 57% of the SDS that triggered events in Montafon and Pitztal occurred in July, followed by Defereggental (50%), Gailtal and the Paltental (each 40%), and the most eastern watershed Feistritzal (33%). The Feistritzal, where the most rainfall per year occurs in June, is the only region where August becomes the most frequent month for SDS trigger (44%), by having one SDS event day more than July. LLR mostly spread over the season from March to November, without showing a general preference for any month. The highest dominance of LLR trigger is observed in the Pitztal, with a fraction of about 60% in July.

The improved methodology of trigger type determination compared to our recent work in Prenner et al. (2018) (all precipitation zones are considered instead of the concerned precipitation zone as described in the Methodology Section) resulted in deviating trigger type assignments for the Montafon region: SDS changed to LLR on the 26th July 1967, SM changed to SDS on 10th June 1970, and LLR changed to SDS on 4th Apr 1978.

4.3. Watershed states at event days

Soil moisture at the beginning of each event day (Fig. 6) as well as measured precipitation on each event day (Fig. 7) are quite different across the regions, per trigger type and between debris flows and fluvial flows. We found statistically significant differences in median soil moisture per trigger class (p -value of Wilcoxon rank sum test $< 5\%$) for the regions Montafon, Gailtal, and Paltental. Here initial relative soil moisture at event days is highest for SM triggered events (median/standard deviation: 0.73/0.07, 0.58/0.01, 0.59/0.13), followed by LLR (0.61/0.07, 0.58/0.11, 0.58/0.07) and lowest for SDS (0.50/0.1, 0.44/0.16, 0.45/0.06). This finding was not confirmed for the regions Pitztal, Defereggental and Feistritzal ($p > 5\%$).

The difference between fluvial flows and debris flows within the same trigger class is marginal. The biggest difference was detected in

Table 2

Median (5th/95th) calibration and validation model performance for the sampled 100 model parameter sets for each study region. NSE = Nash Sutcliffe efficiency of flow, logNSE = Nash Sutcliffe efficiency of logarithmic flow VE = Volumetric Efficiency, FDNSE = Nash Sutcliffe efficiency of flow duration curve, D_E = Euclidian distance of all before mentioned variables.

Region	NSE	logNSE	VE	FDNSE	D_E
	Calibration	Calibration	Calibration	Calibration	Calibration
	Validation	Validation	Validation	Validation	Validation
Montafon	0.73 (0.69/0.73)	0.82 (0.79/0.83)	0.73 (0.69/0.76)	0.95 (0.94/0.97)	0.43 (0.40/0.49)
Pitztal	0.73 (0.68/0.74)	0.83 (0.80/0.84)	0.76 (0.73/0.78)	0.88 (0.83/0.92)	0.41 (0.38/0.50)
Defereggental	0.89 (0.85/0.90)	0.94 (0.80/0.94)	0.81 (0.69/0.83)	0.98 (0.95/0.99)	0.23 (0.21/0.40)
Gailtal	0.87 (0.72/0.89)	0.92 (0.82/0.94)	0.82 (0.69/0.84)	0.96 (0.87/0.98)	0.24 (0.20/0.48)
Paltental	0.89 (0.85/0.90)	0.95 (0.86/0.96)	0.79 (0.68/0.82)	0.99 (0.96/1.00)	0.24 (0.21/0.38)
Feistritzal	0.91 (0.86/0.93)	0.92 (0.74/0.93)	0.77 (0.66/0.80)	0.94 (0.82/0.98)	0.26 (0.22/0.48)
	0.70 (0.67/0.71)	0.88 (0.87/0.89)	0.78 (0.76/0.79)	0.87 (0.83/0.91)	0.42 (0.39/0.46)
	0.90 (0.88/0.91)	0.93 (0.92/0.93)	0.84 (0.81/0.86)	0.94 (0.91/0.96)	0.21 (0.19/0.26)
	0.70 (0.64/0.71)	0.71 (0.65/0.71)	0.74 (0.70/0.76)	0.99 (0.98/0.99)	0.50 (0.47/0.59)
	0.84 (0.80/0.86)	0.88 (0.85/0.90)	0.81 (0.76/0.84)	0.97 (0.86/0.99)	0.27 (0.24/0.37)
	0.78 (0.74/0.78)	0.79 (0.69/0.80)	0.80 (0.78/0.81)	0.97 (0.96/0.99)	0.36 (0.35/0.46)
	0.56 (0.53/0.60)	0.81 (0.75/0.82)	0.79 (0.76/0.80)	0.68 (0.63/0.76)	0.61 (0.54/0.69)

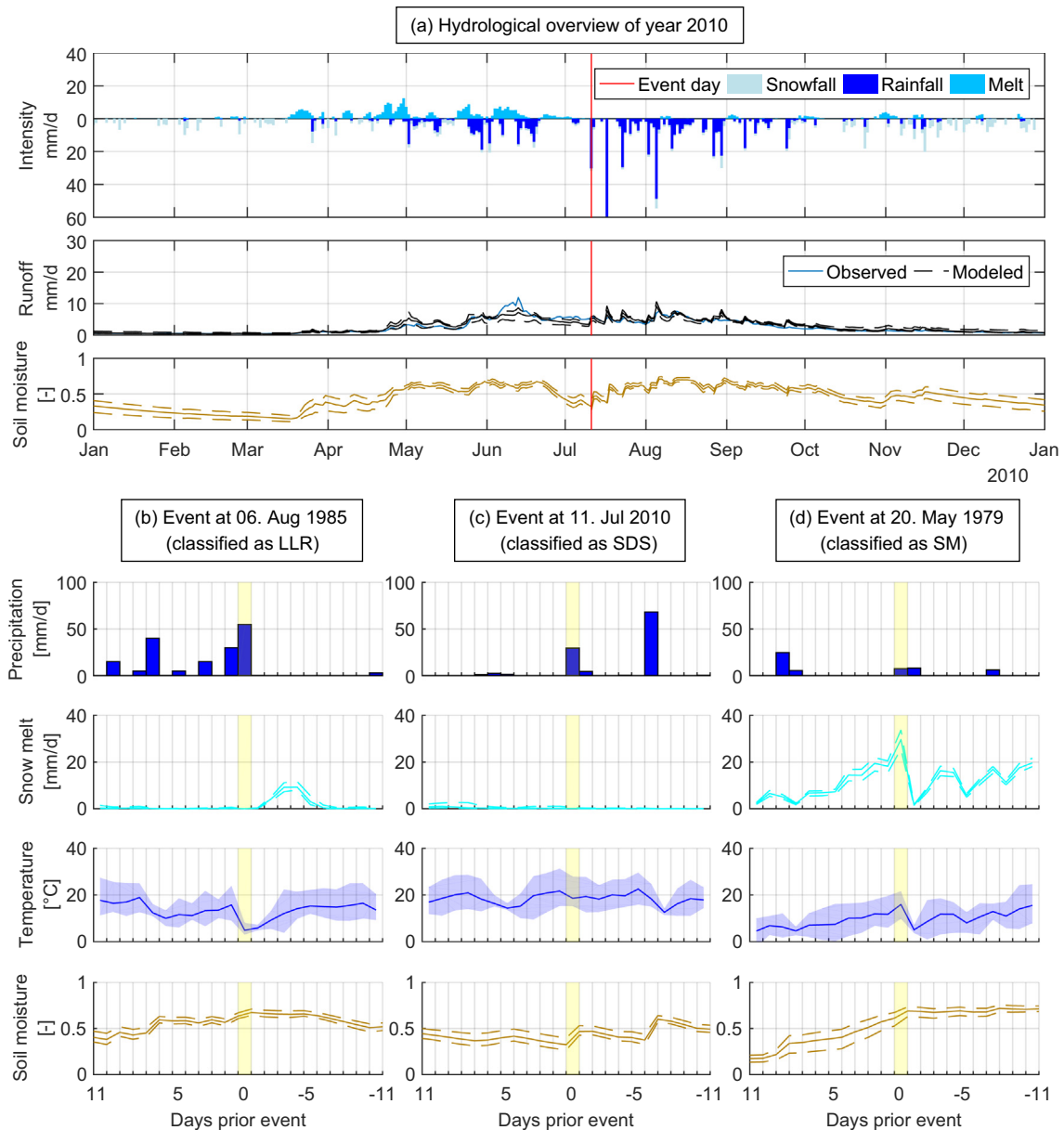


Fig. 3. Hydrological overview of the debris flow event year 2010 of the study region Pitztal (a) as well as three different watershed regimes (which indicate different triggers) at the occurrence of torrential events. The event on 6. August 1976 is interpreted to be triggered by LLR due to a rise of soil moisture caused by ongoing rainfall together with decreasing air temperature to a low level (b). The event on 11. July 2010 is considered to be triggered by a SDS due to a drying up soil on the preceding days driven by evapotranspiration and high temperatures as well as rainfall input on a big span of air temperature at the event day (c). The event on 20 May 1979 is assumed to be triggered by intense SM, facilitated by a high soil moisture level due to ongoing snow melt in the prior days (d).

the region Defereggental, where soil moisture for LLR that triggered fluvial flows (0.73/0.07) was higher than for debris flows (0.56/0.09) with a significance level of $p < 5\%$. A similar trend but with no statistical significance ($p > 5\%$) that fluvial flows are more expected at higher soil pre-saturation compared to debris flow, were observed in Montafon (for trigger type SDS), Pitztal (for trigger type LLR), and the Feistritzal (for trigger types LLR and SDS).

Event day precipitation (Fig. 7) was not directly considered as criterion for the trigger type identification (see Fig. 2 for the criteria) and is therefore an independent variable for the analysis (also not for soil moisture since precipitation affects soil water level at the end of the day and not at the beginning). Results show that median observed precipitation at the event days is significantly higher when LLR was identified as trigger than it was with SDS in the Montafon, Pitztal and Gaital ($p < 5\%$). Regions Defereggental and Feistritzal show the same tendency. This means that LLR triggers, which typically feature higher

antecedent soil moisture levels than SDS, additionally receive higher precipitation input totals compared to SDS. This may be true on a regional and daily time scale, but also highlights the importance of local, high-intensity rainfall events that may deliver relatively small rainfall totals within a short period of time (or have not been measured).

Other than for soil moisture, we found a statistically significant difference ($p < 5\%$) between debris flows and fluvial flows regarding their event day precipitation input when they were triggered by either SDS (median/standard deviation: 11.4/24.9 mm d⁻¹ vs. 25.4/44 mm d⁻¹) or SM (0.1/2.4 mm d⁻¹ vs. 46.1 d⁻¹/34.8 mm d⁻¹) over all study regions. However, LLR triggered fluvial flows (44.8/34.4 mm d⁻¹) and debris flows (23.4/39.6 mm d⁻¹) receive a similar precipitation on event day ($p > 5\%$). Interestingly, the Feistritzal, which is the flattest and lowest-located study region (451–1593 m a.s.l.) and has the densest precipitation network (38 km² per station), shows an opposite but no significant pattern at $p > 5\%$. There, the

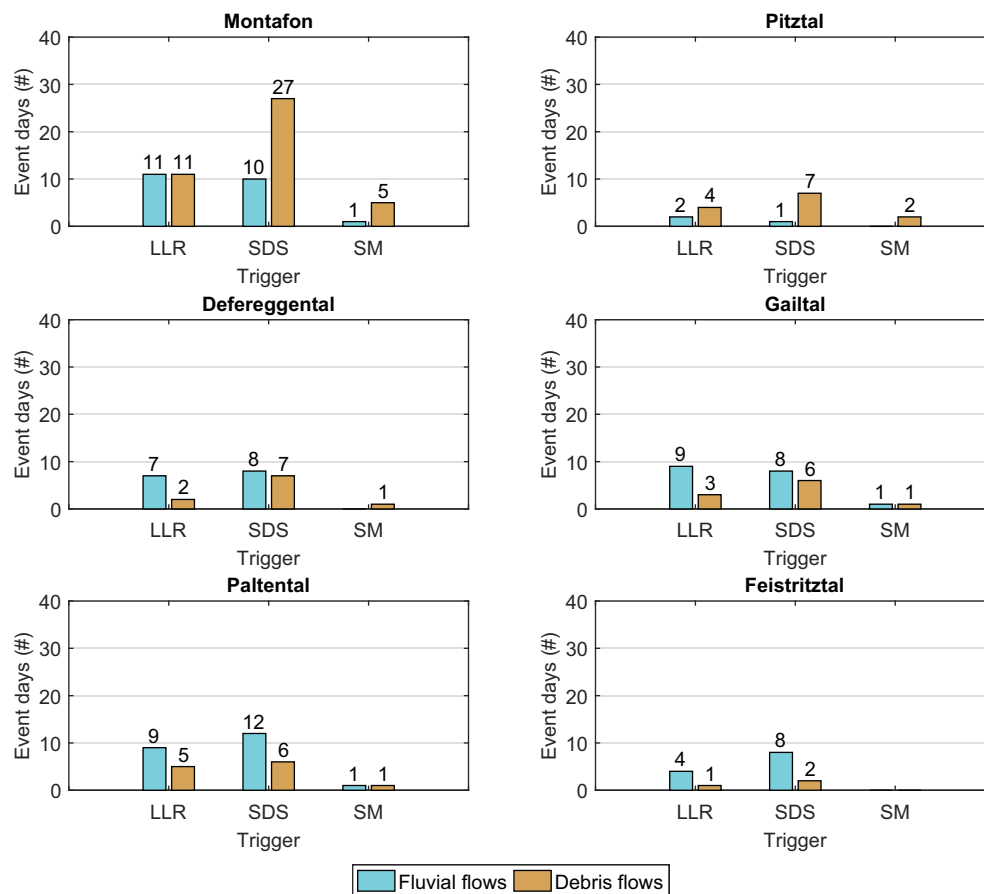


Fig. 4. Number of event days (at least one event occurred) in the six study regions, separated between fluvial flows and debris flows.

occurred debris flows required a higher median precipitation (LLR: 94.0/0.0 mm d⁻¹, SDS: 110.2/68 mm d⁻¹) than the registered fluvial flows (LLR: 63.2/31.0 mm d⁻¹, SDS: 60.0/39.4 mm d⁻¹).

4.4. Temporal development of watershed states

Debris flows and damage causing fluvial flows, occur irregularly and are thus seen as exceptional phenomena. In this section, we analyze whether the week (7 days) preceding the event is somehow extraordinary compared to all other 7-day periods of the event years. Fig. 8 shows exceedance probabilities of daily station precipitation sums (Fig. 8a), mean soil moisture (Fig. 8b), runoff (Fig. 8c) and evapotranspiration (Fig. 8d) in five bins of exceedance probability (0%–20%, 20%–40%, 40%–60%, 60%–80% and 80%–100%) for each trigger type. By a large majority, 71% (median value) of the events triggered by LLR occurred, little surprisingly, in the rainiest periods of the respective years (0%–20% of the periods are more precipitation intense). In contrast, SDS initiated events show a considerably weaker preference to occur the rainiest season with 35%, closely followed by the second rainiest season with a fraction of 31%. Generally, the importance for SDS is higher in the drier periods than for LLR. The role of precipitation for SM triggered events is more diverse. Most of the events occur to the same fraction of 31% in the second rainiest as well as in the second driest period. Interestingly, no event was triggered at moderately rainy conditions (exceedance probability bin 40%–60%). This may indicate a separation between events which are triggered by rain on snow (the two rainiest classes) and such that are initiated purely by intense snow melt (the two rainfall poorest classes).

A very high 7-day mean soil moisture is important for 77% of the SM triggered events. Events triggered by LLR, which build up a gradual soil moisture because of ongoing rainfall, occur only to a fraction of each 39%

in the two most saturated periods of a year (0%–20% and 20%–40% exceedance probability). With SDS triggered events, soil moisture distributes almost to the same fraction (27%, 29%, 27%) over the three most saturated bins (0%–20%, 20%–40%, 40%–60%). This finding supports earlier studies that showed that convective events can start over both, dry and wet soils (Ford et al., 2015; Mostbauer et al., 2018) and may be important to consider when applying antecedent rainfall models to forecast debris flow initiation (Crozier, 1999; Glade et al., 2000).

Indicating generally wet conditions, the highest weekly runoff sums are observed prior to torrential events across all triggers (LLR 56%, SDS 50%, SM 54%). Reduced prior runoff sums also decrease event occurrence probability except for SDS triggers. When 7-day runoff sums are in an average range (exceedance probability 40%–60%), still 24% of the SDS initiated events occur within this period, while at the same conditions the fraction of LLR and SM triggered events amounts only to 4% and 8%, respectively.

The potential evapotranspiration at times of geomorphological events was computed after Hargreaves and Samani (1982) and contains information about the incoming solar energy. As expected, 62% of the SDS events occur in the period with highest magnitudes of potential evapotranspiration within the event year, followed by the SM triggered events with a fraction of 54%. LLR, which are assumed to have a broad, stratiform cloud cover (Rulfová and Kyseľ, 2013) and block incoming solar energy for evapotranspiration, triggered most of the events (48%) at the magnitudes of the second highest bin (20%–40%).

4.5. Geomorphic influence on trigger conditions

While the formation of a weather condition that becomes a trigger (LLR, SDS, SM) for torrential flows can be perceptible at a regional scale (Prenner et al., 2018), in particular the initiation of debris flows

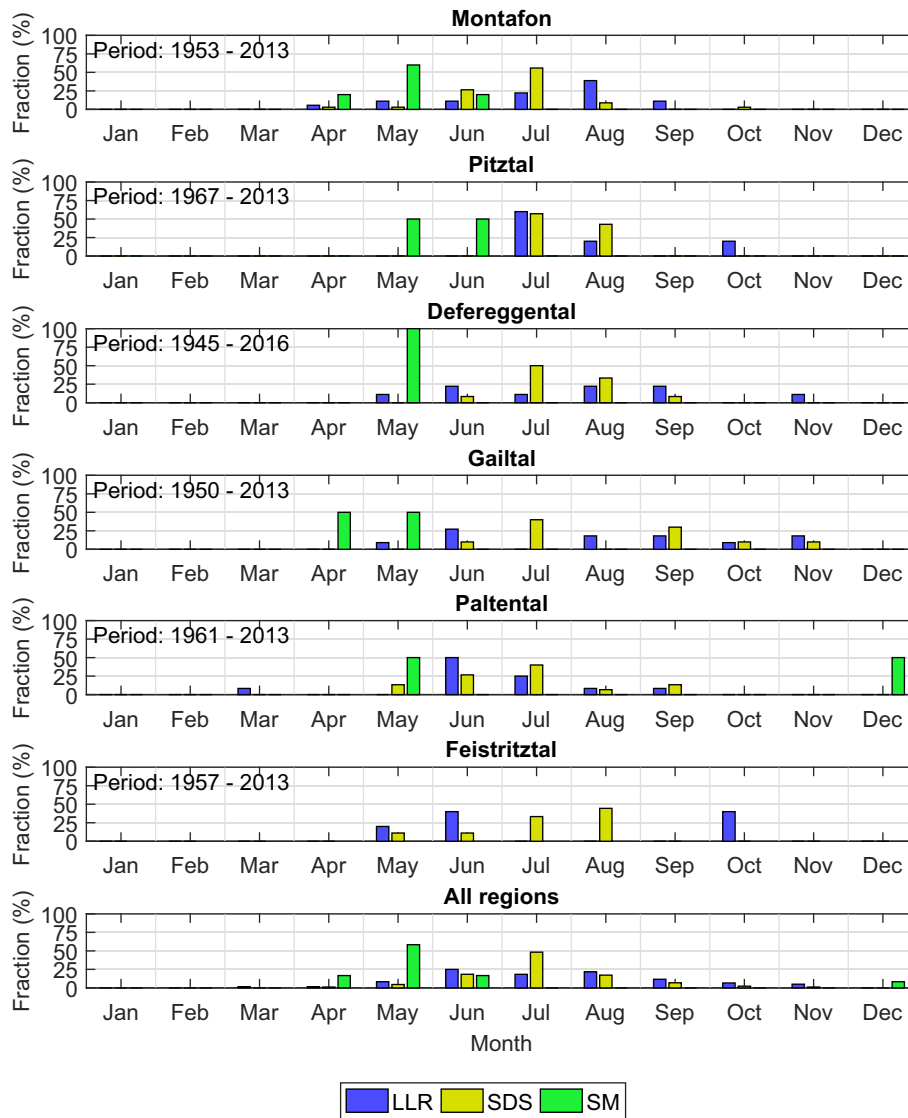


Fig. 5. Temporal distribution of triggers LLR, SDS and SM in all study regions.

depends a lot on local affects like channel erosion, bank or bed failure, or hillslope processes. In this section, we combine the two scales, the precipitation zone and sub-watershed-scale, to investigate whether a trigger type preferentially initiates debris flows and fluvial flows in different sub-watersheds (i.e. torrential watersheds in a study region).

4.5.1. Relief

The relationship between trigger type and the relief of the sub-watersheds, expressed by the Melton Ruggedness Number (MRN), is displayed in Fig. 9. Considering all types of torrential process (fluvial flows and debris flows), there is a significant difference ($p < 5\%$) between SM triggered events, which occurred in rather rugged sub-watersheds (i.e. median/standard deviation of MRN: 1.12/0.46), and LLR triggered events, which are less rugged (0.60/0.45). The difference between the MRN of sub-watersheds triggered by LLR and SDS is statistically insignificant ($p = 0.09$).

When we differentiate between process types, we find that fluvial flows are typically triggered in sub-watersheds with lower median MRN (LLR: 0.48/0.38, SDS: 0.62/0.39, SM: 0.54/0.40) compared to those experiencing debris flows (LLR: 0.79/0.38, SDS: 0.87/0.39, SM: 1.22/0.40), independent of trigger type on a $p < 0.08$ significance level.

4.5.2. Aspect

To further investigate the role of aspect (north, east, south, west), we test if the different trigger types (LLR, SDS, or SM) have a preferential sub-watershed aspect where they initiated torrential events. Fig. 10 shows all surveyed sub-watersheds per study region according to their general slope aspect and the MRN. As seen by the gray point distribution, the slopes of the sub-watersheds of the regions Defereggental, Gailtal and Feistritzal are oriented primarily towards north and south, while in the Pitztal orientation towards the east and west dominates. The regions Montafon and the Paltental have a more diverse structure and sub-watersheds are more homogeneously oriented into all directions. All sub-watersheds that experienced at least one debris flow or fluvial flow event are marked in Fig. 10 following a color code according to their trigger type as well as process type.

A Bayesian analysis is used to quantify the effect of the aspect of the sub-watersheds for the different trigger conditions. More specifically, we determined the probability $P(A|T)$ that a certain sub-watershed with aspect A is experienced a debris flow or fluvial flow event, which was initiated by trigger T.

From the prior distribution of sub-watershed aspects of the Gailtal that triggered events, we expect that 82.5% of the events are

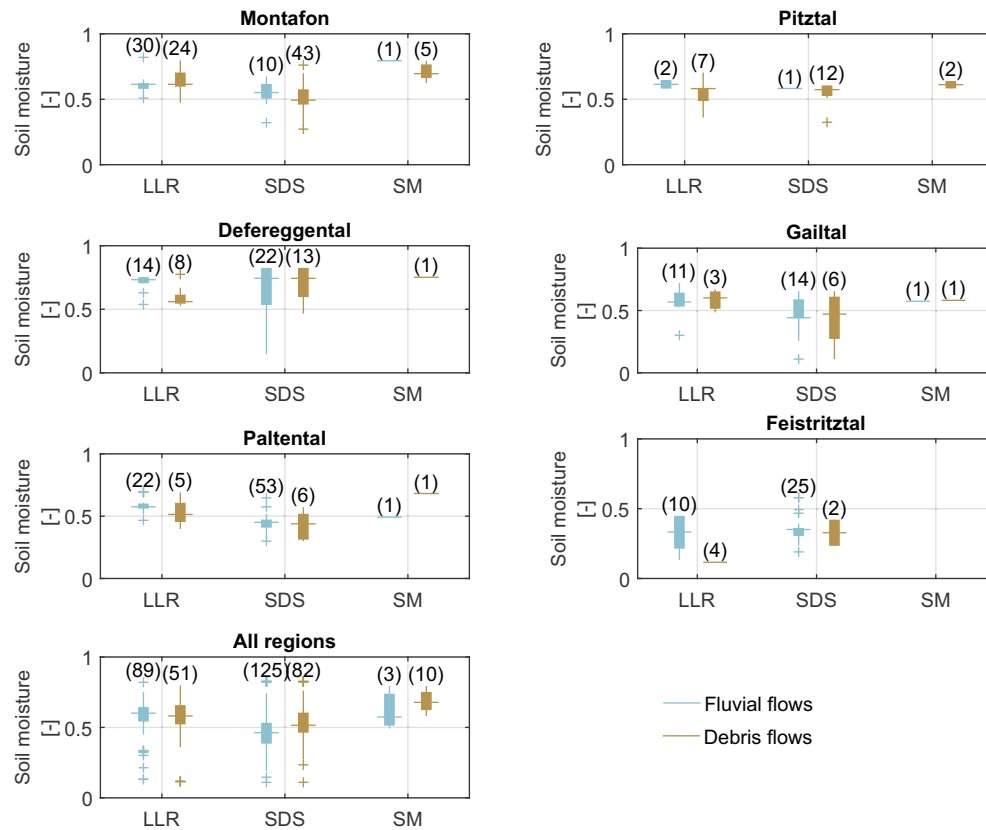


Fig. 6. Initial soil moisture on the event day in the six study regions for each trigger type and torrential process type (fluvial flow or debris flows). The number in brackets displays the number of torrential events in a group.

triggered at southern oriented and 17.5% at northern faced sub-watersheds (Fig. 11). However, when we include information about the trigger type of the events, we obtain the updated posterior probability $P(A|T)$ that all of the events (100%) triggered by LLR or SM occur in western orientated sub-watersheds. Only SDS could initiate events in the northern aligned sub-watersheds with a probability of 30.5%. Southern exposed sub-watersheds are affected by the remaining fraction of 69.5%. A similar situation can be seen in the Pitztal region, where all LLR events occur on western aspects. SDS and SM initiated events, in contrast, were triggered on both, western (SDS: 92.3%, SM: 50.0%) and eastern (SDS: 7.7%, SM: 50.0%) aligned sub-watersheds.

A more diverse picture emerges for the Montafon region, where the aspects of the event producing torrents are more equally distributed (west: 31.5%, north: 26.8%, east: 22.8% and south: 18.9%). Although we know from prior knowledge that western exposed sub-watersheds cause most likely events, this changes for LLR triggered events, which preferentially occur in northern aligned sub-watersheds (35.6%), followed by eastern aspects (29.1%). The western direction is ranked only with a posterior probability of 24.7%. On the other side, SDS triggered events are most probable on western (38.5%) and southern aspects (27.8%), in accordance with the prior information. SM triggered events are almost equally expectable on eastern and western (33.1% and 32.3%) as well as southern and northern watersheds (18.1% and 16.3%). A similar constellation is observed for the Feistritzal region, where the prior distribution (trigger at northern aspect most likely) changes when trigger type information is included (trigger at southern aspect most likely through LLR). In the regions Defereggental and Paltental, additional trigger information could not improve the prior expectation on affected aspects.

5. Discussion

5.1. Uncertainties of trigger type determination

The role of trigger types strongly varies over the seasons as shown in Fig. 5. In general, these findings are in accordance with the work from Stoffel (2010) and Stoffel et al. (2011) who analyzed air pressure data in the Swiss Ritigraben to conclude on the storm type. There, the majority of the events (82%) were connected to high pressure systems (i.e. SDS) which were triggered primarily in July and August. The remaining events (18%) occurred under presence of low pressure systems (that correspond to advective LLR) throughout the whole debris flow season between June to September. A conclusion for SM triggered events or its influence of initiating events could not be quantified from using air pressure data only.

We checked our classification for plausibility, by comparing the determined trigger with weather reports from the Austrian Central Institute for Meteorology and Geodynamics (ZAMG), which are available from 1999 (a summary was attached to the classification result in supplementary material C). Only two event days (17th Jul 2003 in Pitztal and 27th Sep 2012 in Gailtal) out of the 51 event dates deviate from the reports. The reason may be fast changing weather conditions from high pressure to low pressure systems, spatially heterogeneous conditions, the incomplete characterization of hydro-meteorological conditions by the simplified criteria chosen, or even the need for more trigger types than just LLR, SDS and SM. For example, SDS events that occur on three subsequent days prior to a debris flow event may show similar signals in terms of soil moisture as LLR. When then the difference of temperature and evapotranspiration is weakly pronounced, our method may misclassify the trigger as LLR (Prenner et al., 2018).

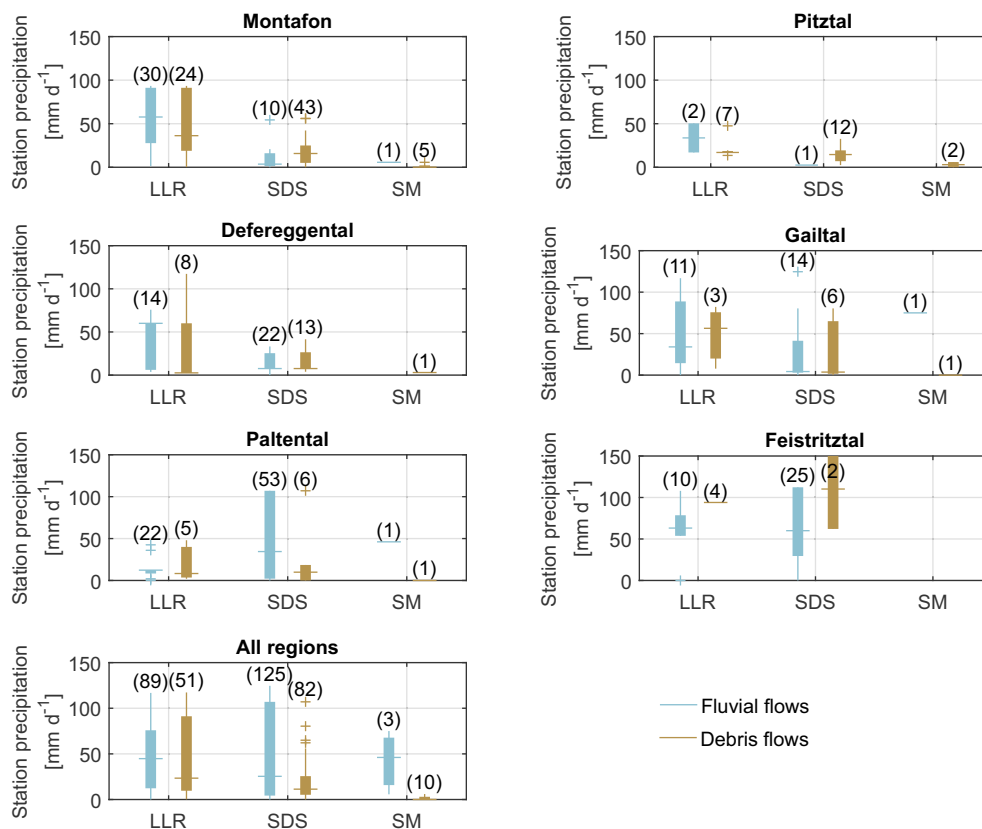


Fig. 7. Observed station precipitation at the event day in the six study regions for each trigger type and torrential process type (fluvial flow or debris flows). The number in brackets displays the number of torrential events in a group.

A demonstration of the complexity and fast changing dynamics of a prevailing trigger displays the situation in the Gailtal region in November 1966 (watershed states are figured in the supplementary material B). For the events on November 3rd, trigger determination resulted in

LLR (determined to a confidence of 97%) and, only one day later, on November 4th a SDS was proposed as trigger (59% confidence). Actually, this rather unexpected classification result was confirmed by weather reports and several event documentations that were available due to

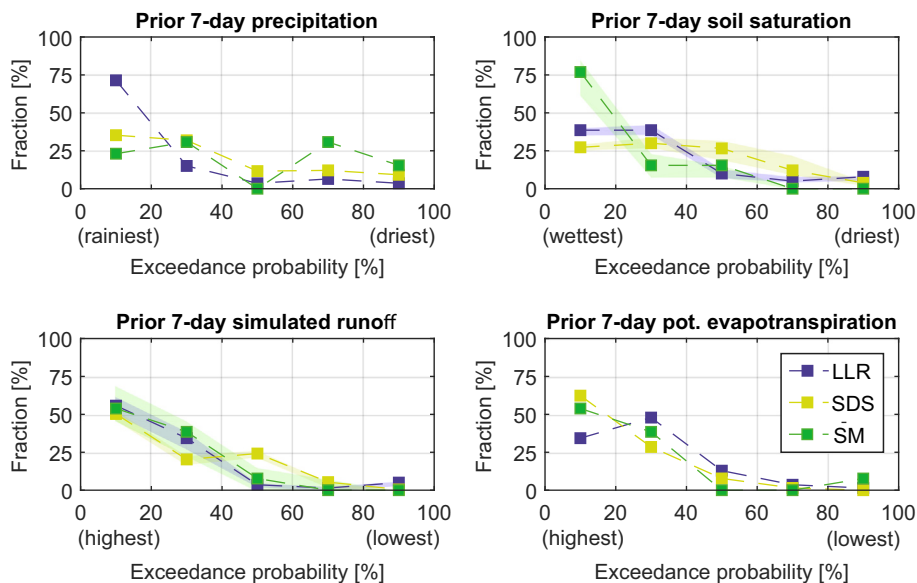


Fig. 8. Exceedance probability of the 7-day condition prior event days compared to all other 7-day conditions in the event year for a) precipitation sum, b) mean soil moisture, c) runoff sum and d) mean potential evapotranspiration.

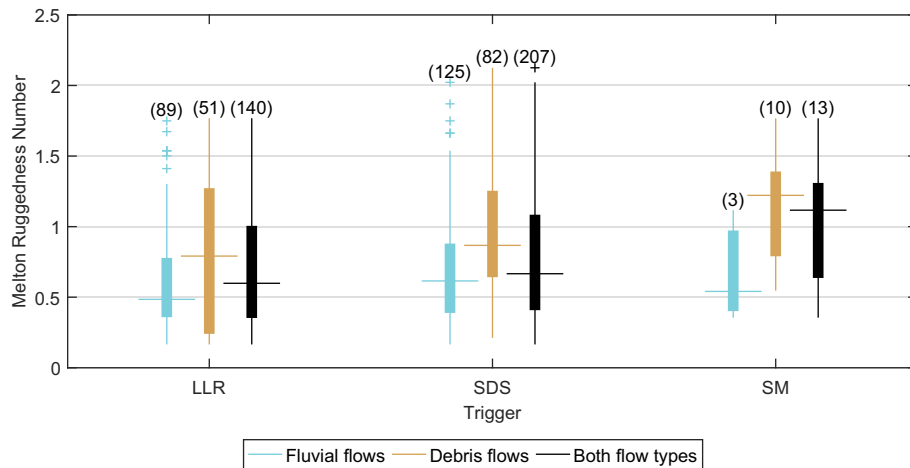


Fig. 9. Melton Ruggedness Number of sub-watersheds (i.e. torrential watersheds) separated by trigger type and process type.

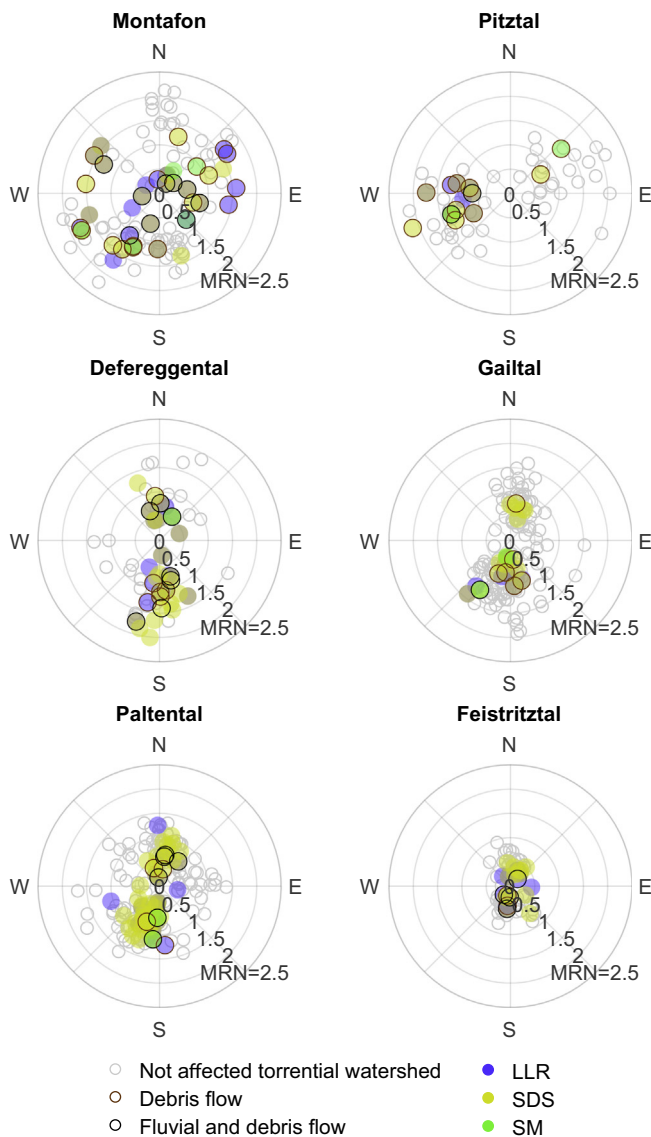


Fig. 10. Overview of the torrential watersheds of the study regions according to their mean aspect and Melton Ruggedness Number (MRN). Colored points mark the sub-watersheds (i.e. torrential watersheds) of a study region which produced torrential events. Gray colored points mark sub-watersheds where no event was registered during the study period.

the catastrophic extent in large parts of Austria. According to Troschl (1967) and Moser (1974), a strong trough (front) moved from the British islands towards the Austria Alps on the 3rd of November. Initial rainfall turned into snow fall in the course of the precipitation event. On the following day, November 4th, strong warm foehn winds initiated thunderstorms and caused snow melt up to high elevations, contributing to the initiation of debris flows and fluvial flows. With our method, the role of snow melt was quantified with a probability of 15% to be the primary trigger. This shows that the initiation of a torrential flow is not always unambiguous to assign to a single specific trigger.

A further uncertainty is the abstraction of diverse trigger conditions in just three classes (LLR, SDS and SM). For example, the 4th of November SDS event in the Gailtal can be described as a winter thunderstorm rather than a classical summer SDS, which occur generally under a different (e.g. cooler) condition (Kitagawa and Michimoto, 1994; Price and Federmesser, 2006). Also, events classified as SM triggered events, occur sometimes in connection with rain and sometimes without rainfall (see Fig. 7). These two circumstances result in considerably different outflow intensities from the snow cover (Singh et al., 1997), what actually represents the available water for torrential event initiation. Such a mixing of different trigger conditions into one class leads to a large scatter of the value space of hydro-meteorological variables what handicaps the deduction of clear distinctions between different trigger types.

Lastly, observed differences in triggering rainfall between LLR and SDS may be epistemic uncertainties from insufficient rainfall observations during convective storms and due to orographic effects (Hrachowitz and Weiler, 2011; Beven et al., 2017a; Beven et al., 2017b).

5.2. Physical initiation mechanism resulting from different trigger conditions and their explanatory power of flow type generation

Generally, one needs to keep in mind that different trigger conditions generate different water intensities (i.e. rainfall intensities from LLR and SDS, melt intensities from SM) that are responsible for the initiation of torrential flows (see Fig. 7; Mostbauer et al., 2018; Prenner et al., 2018). SDS are convective rainfalls which are usually linked to larger precipitation elements (i.e. drops and even hailstone, see Houze (2014)) and a high rainfall intensity over a short time compared to LLR (Rulfová and Kyselý, 2013). The generated water volumes might not suffice (given a low infiltration capacity of the soil) to increase soil pore pressures that cause mass failures on the hillslope or channel bank. Instead, high intensity rainfall may erode and redeposit sediment from the hillslope and the channel leading to the initiation of debris flow surges (Kean et al., 2013; McGuire et al., 2017). Coe et al. (2008) observed high surface runoff resulting from short but intense rainfalls (i.e. SDS) that develop as debris flows in the channel. The same authors

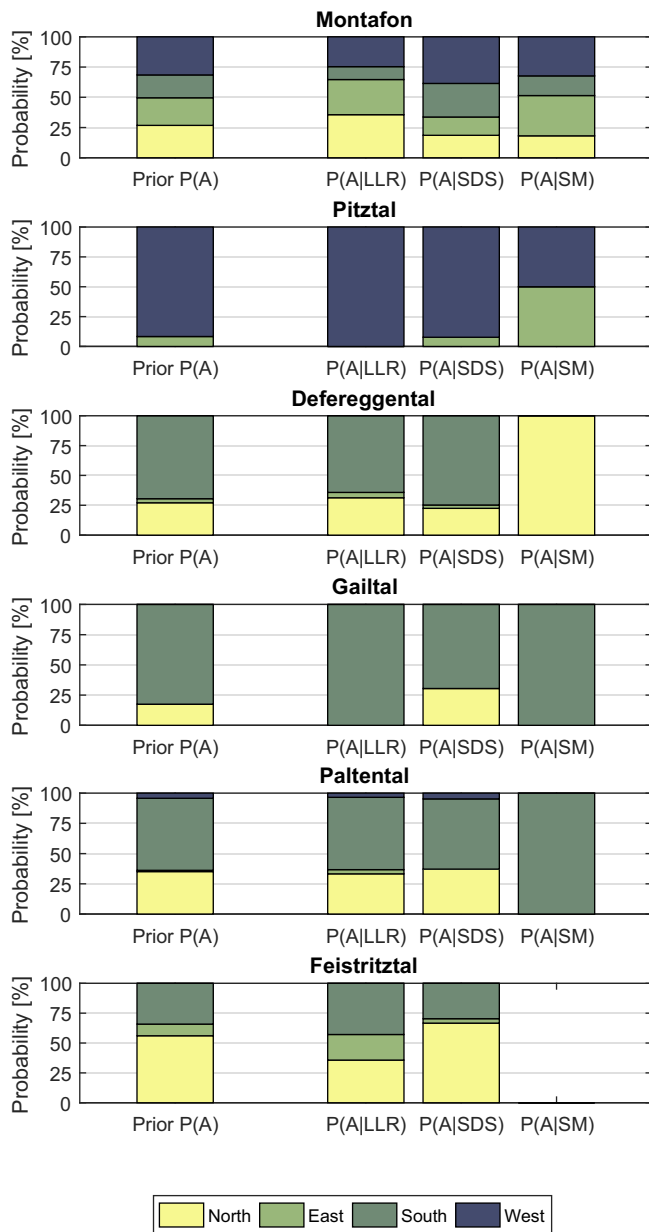


Fig. 11. Prior probability $P(A)$ to observe a torrential watershed exposed to aspect A (north, east, south, west) in the study region and posterior probability $P(A|T)$ that a torrential watershed with mean aspect A is affected by an event triggered by T (LLR = long-lasting rainfall, SDS = short-duration storm, SM = intense snow melt).

report of unsaturated soil moisture conditions before the rainfall started, a situation that we also found in our study regions in connection with SDS (Fig. 6).

LLR events show both, higher soil moisture (Fig. 6) on the event days as well as higher event day precipitation sums (Fig. 7) compared to SDS events, indicating a contrasting soil-mechanical response. The enduring but less intense water input can produce high soil pore fluid pressures on the hillslopes close to channels. Once a critical level is reached, high pore water pressure can cause a local mass failure (Lehmann and Or, 2012) that can further propagate as debris flows (Fan et al., 2017). Stoffel et al. (2011) found that in the Swiss Rätigraben the larger debris flow magnitudes (10^4 to $5 \cdot 10^4 \text{ m}^3$) were observed with advective triggered events (LLR) and the smaller to medium magnitudes with SDS (up to $5 \cdot 10^4 \text{ m}^3$).

According to our finding, there is little evidence that the hydro-meteorological setting of a watershed controls the type of torrential

flow process. We speculate that instead, other factors such as sediment availability, or presence of woody debris may promote the initiation of debris flows in situations where otherwise flood events with or without intensive sediment transport would have occurred. For further analysis, sedimentary and geological data from field measurements should be included to derive stronger evidences on this topic.

5.3. Susceptibility of torrential watersheds to certain trigger types

We found that the consideration of the aspect of the sub-watersheds in a certain region can add substantial information for the identification of the susceptibility for torrential events in dependence of a certain trigger. A reason for the diverging behavior of trigger types may be their specific process characteristics. LLR are usually large stratiform phenomenon based on a frontal, directed movement of air masses (Ahrens, 2011; Houze, 2014; Häckel, 2016) that are affected by topographic effects. Hence, they affect sub-watersheds characterized by a similar directed aspect. In contrast, SDS are convective, strong upward movements of moist air masses with no distinct horizontal movements (Ahrens, 2011; Houze, 2014; Häckel, 2016), and therefore less affected by topography. Both, LLR and SDS processes, can be enhanced through orographic lifting effects (Wastl and Zängl, 2008; Häckel, 2016). The limited number of SM initiated events in our study region does not allow drawing any conclusions about preferential aspects.

6. Conclusions

In this study, we analyzed six mountain regions to obtain a holistic picture of the variability of hydro-meteorological trigger conditions of documented debris flows and fluvial flows (damage causing flash floods with or without intensive bedload transport). The selected study regions cover very different climatic and topographic settings in the eastern Alps. We use hydrologic state and flux variables on a daily time scale to classify the trigger of such events into long-lasting rainfall (LLR), short-duration storm (SDS), and snow melt (SM). Additionally, we relate our findings to several basic geomorphological characteristics (Melton Ruggedness Number and mean aspect) of the sub-watersheds in which these torrential processes occurred. With regard to our expectations, the findings of this study are summarized as follows:

Hypothesis 1. “Hydro-meteorological trigger conditions generally differ for debris flows and fluvial flow processes”:

- On a daily time scale, fluvial flows require a higher precipitation input than debris flows when they are triggered by SDS or SM but not by LLR (Fig. 7). For soil moisture at the beginning of the event day, we cannot find any significant difference between fluvial flows and debris flows and any trigger (Fig. 6).
- Measured precipitation on the event day is significantly different for the trigger classes LLR, SDS, and SM (Fig. 7).
- Both, the initial soil moisture as well as the rainfall on the event day, is higher for events associated with LLR than with SDS across all study regions (Figs. 6 and 7).

Hypothesis 2. “Trigger conditions vary between different regions in the Austrian Alps”:

- Initial soil moisture and event day precipitation sums strongly vary across the regions for the same trigger type. However, the temporal change of hydrological watershed state before events show similar signals across the regions and allows to draw more general conclusions about the susceptibility of regions to torrential processes (Figs. 6 and 7).

Hypothesis 3. “Trigger conditions vary with geomorphic basin characteristics within the same region”:

- Torrential events initiated by SM occur in sub-watersheds with a significant higher Melton Ruggedness Number compared to LLR. Additionally, there is a tendency that SDS initiates events at slightly higher ruggedness than LLR (Fig. 9).
- LLR exclusively triggered debris flows and fluvial flows in sub-watersheds of a specific aspect in the Gailtal and Pitztal (south and west, respectively). On the contrary, SDS and SM triggered events on multiple oriented sub-watersheds (Figs. 10 and 11).

We conclude that the initiation of torrential processes is connected to various hydro-meteorological conditions and that using trigger type information contributes to a better understanding of the interplay between meteorology, hydrology and geomorphology. Nevertheless, hydro-meteorological information alone is not sufficient to predict the type of torrential process (fluvial or debris flow) expectable from a sub-watershed.

Acknowledgments and data

We thank HD Austria including its subdivisions of Vorarlberg, Tyrol, Carinthia, Styria and Lower Austria, the ZAMG, TIWAG, Voralberger Illwerke AG for supplying the climate and hydrologic datasets. The model runs were performed on the Vienna Scientific Cluster (vsc.ac.at) which we thankfully acknowledge. This project receives financial support from the Austrian Climate and Energy Fund [grant number B464795] and is carried out within the framework of the ‘ACRP’ Programme. Additionally, we would like to thank the two anonymous reviewer for their valuable comments helping to improve the manuscript.

Appendix A. Supplementary data

Supplementary data to this article can be found online at <https://doi.org/10.1016/j.scitotenv.2018.12.206>.

References

- Ahrens, C.D., 2011. *Essentials of Meteorology: An Invitation to the Atmosphere*. 6th ed. Brooks/Cole, Belmont, CA.
- Atkinson, P.M., Massari, R., 1998. Generalised linear modelling of susceptibility to landsliding in the central Apennines, Italy. *Comput. Geosci.* 24 (4), 373–385. [https://doi.org/10.1016/S0098-3004\(97\)00117-9](https://doi.org/10.1016/S0098-3004(97)00117-9).
- Austrian Standards International, 2009. *Protection Works for Torrent Control—Terms and their Definitions as Well as Classification*. Austrian Standards International, Vienna, Austria.
- Ayalew, L., Yamagishi, H., Ugawa, N., 2004. Landslide susceptibility mapping using GIS-based weighted linear combination, the case in Tsugawa area of Agano River, Niigata prefecture, Japan. *Landslides* 1 (1), 73–81. <https://doi.org/10.1007/s10346-003-0006-9>.
- Badoux, A., Turowski, J.M., Mao, L., Mathys, N., Rickenmann, D., 2012. Rainfall intensity-duration thresholds for bedload transport initiation in small alpine watersheds. *Nat. Hazards Earth Syst. Sci.* 12 (10), 3091–3108. <https://doi.org/10.5194/nhess-12-3091-2012>.
- Ballesteros Cánovas, J.A., Stoffel, M., Corona, C., Schraml, K., Gobiet, A., Tani, S., ... Kaitna, R., 2016. Debris-flow risk analysis in a managed torrent based on a stochastic life-cycle performance. *Sci. Total Environ.* 557–558, 142–153. <https://doi.org/10.1016/j.scitotenv.2016.03.036>.
- Bayes, T., Price, R., 1763. An essay towards solving a problem in the doctrine of chances. By the late Rev. Mr. Bayes, F. R. S. communicated by Mr. Price, in a letter to John Canton, A. M. F. R. S. *Philos. Trans.* 1683–1775, 370–418.
- Berti, M., Martina, M.L.V., Franceschini, S., Pignone, S., Simoni, A., Pizzoli, M., 2012. Probabilistic rainfall thresholds for landslide occurrence using a Bayesian approach. *J. Geophys. Res. Earth Surf.* 117 (F4). <https://doi.org/10.1029/2012JF002367> (n/a–n/a).
- Beven, K.J., Almeida, S., Aspinall, W.P., Bates, P.D., Blazkova, S., Borgomeo, E., ... Wilkins, K.L., 2017a. Epistemic uncertainties and natural hazard risk assessment. 1. A review of different natural hazard areas. *Nat. Hazards Earth Syst. Sci. Discuss.*, 1–53 <https://doi.org/10.5194/nhess-2017-250>.
- Beven, K.J., Aspinall, W.P., Bates, P.D., Borgomeo, E., Goda, K., Hall, J.W., ... Watson, M., 2017b. Epistemic uncertainties and natural hazard risk assessment. 2. What should constitute good practice? *Nat. Hazards Earth Syst. Sci. Discuss.*, 1–25 <https://doi.org/10.5194/nhess-2017-251>.
- Bogaard, T.A., Greco, R., 2016. Landslide hydrology: from hydrology to pore pressure: landslide hydrology. *Wiley Interdiscip. Rev. Water* 3 (3), 439–459. <https://doi.org/10.1002/wat2.1126>.
- Borga, M., Stoffel, M., Marchi, L., Marra, F., Jakob, M., 2014. Hydrogeomorphic response to extreme rainfall in headwater systems: flash floods and debris flows. *J. Hydrol.* 518, 194–205. <https://doi.org/10.1016/j.jhydrol.2014.05.022>.
- Capitani, M., Ribolini, A., Bini, M., 2013. The slope aspect: a predisposing factor for landsliding? *Comput. Rendus Geosci.* 345 (11–12), 427–438. <https://doi.org/10.1016/j.crte.2013.11.002>.
- Coe, J.A., Kinner, D.A., Godt, J.W., 2008. Initiation conditions for debris flows generated by runoff at chalk cliffs, central Colorado. *Geomorphology* 96 (3–4), 270–297. <https://doi.org/10.1016/j.geomorph.2007.03.017>.
- Criss, R.E., Winston, W.E., 2008. Do Nash values have value? Discussion and alternate proposals. *Hydrol. Process.* 22 (14), 2723–2725. <https://doi.org/10.1002/hyp.7072>.
- Crozier, M.J., 1999. Prediction of rainfall-triggered landslides: a test of the antecedent water status model. *Earth Surf. Process. Landf.* 24 (9), 825–833. [https://doi.org/10.1002/\(SICI\)1096-9837\(199908\)24:9<825::AID-ESP14>3.0.CO;2-M](https://doi.org/10.1002/(SICI)1096-9837(199908)24:9<825::AID-ESP14>3.0.CO;2-M).
- Dall’Amico, M., Hornsteiner, M., 2006. A simple method for estimating daily and monthly mean temperatures from daily minima and maxima. *Int. J. Climatol.* 26 (13), 1929–1936. <https://doi.org/10.1002/joc.1363>.
- Ellenberg, H., Leuschner, C., Dierschke, H., 2010. *Vegetation Mitteleuropas mit den Alpen: in ökologischer, dynamischer und historischer Sicht; 203 Tabellen* (6., vollst. neu bearb. und stark erw. Aufl.). Ulmer, Stuttgart.
- Euser, T., Hrachowitz, M., Winsemius, H.C., Savenije, H.H.G., 2015. The effect of forcing and landscape distribution on performance and consistency of model structures. *Hydrol. Process.* 29 (17), 3727–3743. <https://doi.org/10.1002/hyp.10445>.
- Fan, L., Lehmann, P., McArdell, B., Or, D., 2017. Linking rainfall-induced landslides with debris flows runoff patterns towards catchment scale hazard assessment. *Geomorphology* 280, 1–15. <https://doi.org/10.1016/j.geomorph.2016.10.007>.
- Ford, T.W., Rapp, A.D., Quiring, S.M., Blake, J., 2015. Soil moisture–precipitation coupling: observations from the Oklahoma Mesonet and underlying physical mechanisms. *Hydrol. Earth Syst. Sci.* 19 (8), 3617–3631. <https://doi.org/10.5194/hess-19-3617-2015>.
- Fuchs, S., Röthlisberger, V., Thaler, T., Zischg, A., Keiler, M., 2017. Natural hazard management from a coevolutionary perspective: exposure and policy response in the European alps. *Ann. Am. Assoc. Geogr.* 107 (2), 382–392. <https://doi.org/10.1080/24694452.2016.1235494>.
- Galli, M., Ardizzone, F., Cardinali, M., Guzzetti, F., Reichenbach, P., 2008. Comparing landslide inventory maps. *Geomorphology* 94 (3–4), 268–289. <https://doi.org/10.1016/j.geomorph.2006.09.023>.
- Gao, H., Hrachowitz, M., Fenicia, F., Gharari, S., Savenije, H.H.G., 2014. Testing the realism of a topography-driven model (FLEX-topo) in the nested catchments of the upper Heihe, China. *Hydrol. Earth Syst. Sci.* 18 (5), 1895–1915. <https://doi.org/10.5194/hess-18-1895-2014>.
- Gao, H., Ding, Y., Zhao, Q., Hrachowitz, M., Savenije, H.H., 2017. The importance of aspect for modelling the hydrological response in a glacier catchment in central Asia. *Hydrol. Process.* 31 (16), 2842–2859.
- Gharari, S., Hrachowitz, M., Fenicia, F., Savenije, H.H.G., 2011. Hydrological landscape classification: investigating the performance of HAND based landscape classifications in a central European meso-scale catchment. *Hydrol. Earth Syst. Sci.* 15 (11), 3275–3291. <https://doi.org/10.5194/hess-15-3275-2011>.
- Glade, T., Crozier, M., Smith, P., 2000. Applying probability determination to refine landslide-triggering rainfall thresholds using an empirical “antecedent daily rainfall model”. *Pure Appl. Geophys.* 157 (6–8), 1059–1079.
- Gregoretti, C., Fontana, G.D., 2008. The triggering of debris flow due to channel-bed failure in some alpine headwater basins of the Dolomites: analyses of critical runoff. *Hydrol. Process.* 22 (13), 2248–2263. <https://doi.org/10.1002/hyp.6821>.
- Guzzetti, F., Peruccacci, S., Rossi, M., Stark, C.P., 2008. The rainfall intensity–duration control of shallow landslides and debris flows: an update. *Landslides* 5 (1), 3–17. <https://doi.org/10.1007/s10346-007-0112-1>.
- Häckel, H., 2016. *Meteorologie* (8., vollständig überarbeitete und erweiterte Auflage). Verlag Eugen Ulmer, Stuttgart.
- Hargreaves, G.H., Samani, Z.A., 1982. Estimation of potential evapotranspiration. *J. Irrig. Drain. Div.* 108 (IR3), 223–230. *Proceedings of the American Society of Civil Engineers*.
- Heiser, M., Scheidl, C., Eisl, J., Spangl, B., Hübl, J., 2015. Process type identification in torrential catchments in the eastern Alps. *Geomorphology* 232, 239–247. <https://doi.org/10.1016/j.geomorph.2015.01.007>.
- Hock, R., 2003. Temperature index melt modelling in mountain areas. *J. Hydrol.* 282 (1–4), 104–115. [https://doi.org/10.1016/S0022-1694\(03\)00257-9](https://doi.org/10.1016/S0022-1694(03)00257-9).
- Houze, R.A., 2014. *Cloud Dynamics*. Second edition. Academic Press is an imprint of Elsevier, Amsterdam; New York.
- Hrachowitz, M., Weiler, M., 2011. Uncertainty of precipitation estimates caused by sparse gauging networks in a small, mountainous watershed. *J. Hydrol. Eng.* 16 (5), 460–471. [https://doi.org/10.1061/\(ASCE\)HE.1943-5584.0000331](https://doi.org/10.1061/(ASCE)HE.1943-5584.0000331).
- Hrachowitz, M., Fovet, O., Ruiz, L., Euser, T., Gharari, S., Nijzink, R., ... Gascuel-Oudoux, C., 2014. Process consistency in models: the importance of system signatures, expert knowledge, and process complexity. *Water Resour. Res.* 50 (9), 7445–7469. <https://doi.org/10.1002/2014WR015484>.
- Hübl, J., Totschnig, R., Scheidl, C., 2008a. *Historische Ereignisse Band 1: Auswertung von Wildbach Schadereignissen bis 1891 auf Basis der “Brixner Chronik”* (IAN Report No. 111). Institut für Alpine Naturgefahren, Wien.

- Hübl, J., Totschnig, R., Sitter, F., Mayer, B., Schneider, A., 2008b. Historische Ereignisse Band 2: Auswertung von Wildbach Schadereignissen in Westösterreich auf Grundlage der Wildbachaufnahmeblätter (IAN Report No. 111). Institut für Alpine Naturgefahren, Wien.
- Hübl, J., Totschnig, R., Sitter, F., Schneider, A., Krawtschuk, A., Dosl, G., ... Neckel, N., 2008c. Historische Ereignisse Band 3: Auswertung von Wildbach Schadereignissen in Österreich auf Grundlage der Wildbachaufnahmeblätter (IAN Report No. 111). Institut für Alpine Naturgefahren, Wien.
- Hübl, J., Totschnig, R., Sitter, F., Schneider, A., Krawtschuk, A., 2010. Historische Ereignisse Band 4: Zusammenstellung und Analyse dokumentierter Ereignisse in Österreich bis 2009 (IAN Report No. 111). Institut für Alpine Naturgefahren, Wien.
- Hungr, O., Leroueil, S., Picarelli, L., 2014. The Varnes classification of landslide types, an update. *Landslides* 11 (2), 167–194. <https://doi.org/10.1007/s10346-013-0436-y>.
- Jackson, L.E., Kostaschuk, R.A., MacDonald, G.M., 1987. Identification of debris flow hazard on alluvial fans in the Canadian rocky mountains. *Reviews in Engineering Geology*. vol. 7. Geological Society of America, pp. 115–124. <https://doi.org/10.1130/REG7-p115>.
- Johnson, K.A., Sitar, N., 1990. Hydrologic conditions leading to debris-flow initiation. *Can. Geotech. J.* 27 (6), 789–801.
- Kean, J.W., McCoy, S.W., Tucker, G.E., Staley, D.M., Coe, J.A., 2013. Runoff-generated debris flows: observations and modeling of surge initiation, magnitude, and frequency. *J. Geophys. Res. Earth Surf.* 118 (4), 2190–2207. <https://doi.org/10.1002/jgrf.20148>.
- Kitagawa, N., Michimoto, K., 1994. Meteorological and electrical aspects of winter thunderclouds. *J. Geophys. Res.* 99 (D5), 10713. <https://doi.org/10.1029/94JD00288>.
- Lehmann, P., Or, D., 2012. Hydromechanical triggering of landslides: from progressive local failures to mass release. *Water Resour. Res.* 48 (3). <https://doi.org/10.1029/2011WR010947>.
- Luzi, L., Pergalani, F., 1999. Slope instability in static and dynamic conditions for urban planning: the 'Oltre Po Pavese' case history (Regione Lombardia – Italy). *Nat. Hazards* 20 (1), 26.
- Mader, H., Steidl, T., Wimmer, R., 1996. Abflussregime österreichischer Fließgewässer: Beitrag zu einer bundesweiten Fließgewässertypologie. Umweltbundesamt, Wien.
- Marchi, L., Arattano, M., Deganutti, A.M., 2002. Ten years of debris-flow monitoring in the Moscardo Torrent (Italian Alps). *Geomorphology* 46, 1–2, 1–17. [https://doi.org/10.1016/S0169-555X\(01\)00162-3](https://doi.org/10.1016/S0169-555X(01)00162-3).
- McGuire, L.A., Rengers, F.K., Kean, J.W., Staley, D.M., 2017. Debris flow initiation by runoff in a recently burned basin: is grain-by-grain sediment bulking or en masse failure to blame? *Geophys. Res. Lett.* 44. <https://doi.org/10.1002/2017GL074243>.
- Melton, A., 1957. *An Analysis of the Relations Among Elements of Climate, Surface Properties, and Geomorphology*. Columbia University, New York: Office of Naval Research, Dep. of Geology.
- Merz, R., Blöschl, G., 2003. A process typology of regional floods. *Water Resour. Res.* 39 (12). <https://doi.org/10.1029/2002WR001952>.
- Moser, M., 1974. Analyse der Anbruchsbildung bei den Hochwasserkatastrophen der Jahre 1965 und 1966 im mittleren Lesachtal (Kärnten). *Carinthia II* 163 (83), 179–234.
- Mostbauer, K., Kaitna, R., Prenner, D., Hrachowitz, M., 2018. The temporally varying roles of rainfall, snowmelt and soil moisture for debris flow initiation in a snow-dominated system. *Hydrol. Earth Syst. Sci.* 22 (6), 3493–3513. <https://doi.org/10.5194/hess-22-3493-2018>.
- Nachtnebel, H.P., 2003. *Hydrologischer Atlas Österreichs: HAÖ. Österr. Kunst- und Kulturverl., Wien.*
- Nash, J.E., Sutcliffe, J.V., 1970. River flow forecasting through conceptual models part I – a discussion of principles. *J. Hydrol.* 10 (3), 282–290. [https://doi.org/10.1016/0022-1694\(70\)90255-6](https://doi.org/10.1016/0022-1694(70)90255-6).
- Parajka, J., Merz, R., Blöschl, G., 2005. Regional water balance components in Austria on a daily basis. *Österreichische Wasser- Und Abfallwirtschaft* 57 (3), 43–56. <https://doi.org/10.1007/BF03165611>.
- Patzelt, G., 2015. The Austrian glacier inventory GI 1, 1969. ArcGIS (Shapefile) Format. PANGAEA – Data Publisher for Earth & Environmental Science <https://doi.org/10.1594/PANGAEA.844983>.
- Prenner, D., Kaitna, R., Mostbauer, K., Hrachowitz, M., 2018. The value of using multiple hydro-meteorological variables to predict temporal debris flow susceptibility in an alpine environment. *Water Resour. Res.* <https://doi.org/10.1029/2018WR022985>.
- Price, C., Federmesser, B., 2006. Lightning-rainfall relationships in Mediterranean winter thunderstorms. *Geophys. Res. Lett.* 33 (7). <https://doi.org/10.1029/2005GL024794>.
- Rennó, C.D., Nobre, A.D., Cuartas, L.A., Soares, J.V., Hodnett, M.G., Tomasella, J., Waterloo, M.J., 2008. HAND, a new terrain descriptor using SRTM-DEM: mapping terra-firme rainforest environments in Amazonia. *Remote Sens. Environ.* 112 (9), 3469–3481. <https://doi.org/10.1016/j.rse.2008.03.018>.
- Rolland, C., 2003. Spatial and seasonal variations of air temperature lapse rates in alpine regions. *J. Clim.* 16 (7), 1032–1046.
- Rulfova, Z., Kysely, J., 2013. Disaggregating convective and stratiform precipitation from station weather data. *Atmos. Res.* 134, 100–115. <https://doi.org/10.1016/j.atmosres.2013.07.015>.
- Scheidl, C., Rickenmann, D., 2009. Empirical prediction of debris-flow mobility and deposition on fans. *Earth Surf. Process. Landf.* <https://doi.org/10.1002/esp.1897> (n/a–n/a).
- Sevruck, B., 1997. Regional dependency of precipitation-altitude relationship in the Swiss Alps. In: Diaz, H.F., Beniston, M., Bradley, R.S. (Eds.), *Climatic Change at High Elevation Sites*. Springer Netherlands, Dordrecht, pp. 123–137. https://doi.org/10.1007/978-94-015-8905-5_7.
- Singh, P., Spitzbart, G., Hübl, H., Weinmeister, H., 1997. Hydrological response of snow-pack under rain-on-snow events: a field study. *J. Hydrol.* 202 (1–4), 1–20. [https://doi.org/10.1016/S0022-1694\(97\)00004-8](https://doi.org/10.1016/S0022-1694(97)00004-8).
- Stock, J., Dietrich, W.E., 2003. Valley incision by debris flows: evidence of a topographic signature. *Water Resour. Res.* 39 (4). <https://doi.org/10.1029/2001WR001057>.
- Stoffel, M., 2010. Magnitude–frequency relationships of debris flows – a case study based on field surveys and tree-ring records. *Geomorphology* 116 (1–2), 67–76. <https://doi.org/10.1016/j.geomorph.2009.10.009>.
- Stoffel, M., Bollschweiler, M., Beniston, M., 2011. Rainfall characteristics for periglacial debris flows in the Swiss Alps: past incidences–potential future evolutions. *Clim. Chang.* 105 (1–2), 263–280. <https://doi.org/10.1007/s10584-011-0036-6>.
- Thiessen, A.H., 1911. Precipitation averages for large areas. *Mon. Weather Rev.* 39 (7), 1082–1084.
- Troschl, H., 1967. Die Hochwasserwetterlagen 1965 und 1966. *Interprävent Tagungsbericht*, pp. 18–24.
- Vrugt, J.A., 2016. Markov chain Monte Carlo simulation using the DREAM software package: theory, concepts, and MATLAB implementation. *Environ. Model. Softw.* 75, 273–316. <https://doi.org/10.1016/j.envsoft.2015.08.013>.
- Vrugt, J.A., ter Braak, C.J.F., Clark, M.P., Hyman, J.M., Robinson, B.A., 2008. Treatment of input uncertainty in hydrologic modeling: doing hydrology backward with Markov chain Monte Carlo simulation. *Water Resour. Res.* 44 (12). <https://doi.org/10.1029/2007WR006720> (n/a–n/a).
- Wastl, C., Zängl, G., 2008. Analysis of mountain-valley precipitation differences in the Alps. *Meteorol. Z.* 17 (3), 311–321. <https://doi.org/10.1127/0941-2948/2008/0291>.
- Wilcoxon, F., 1945. Individual comparisons by ranking methods. *Biom. Bull.* 1 (6), 80. <https://doi.org/10.2307/3001968>.
- Yalcin, A., Reis, S., Aydinoglu, A.C., Yomralioglu, T., 2011. A GIS-based comparative study of frequency ratio, analytical hierarchy process, bivariate statistics and logistics regression methods for landslide susceptibility mapping in Trabzon, NE Turkey. *Catena* 85 (3), 274–287. <https://doi.org/10.1016/j.catena.2011.01.014>.